

Lawrence Berkeley National Laboratory

Recent Work

Title

Infrared light curves of type Ia supernovae

Permalink

<https://escholarship.org/uc/item/8mk6t96r>

Authors

Phillips, MM
Krisciunas, K
Suntzeff, NB
[et al.](#)

Publication Date

2003

DOI

10.1007/10828549_25

Peer reviewed

Infrared Light Curves of Type Ia Supernovae

M. M. Phillips¹, K. Krisciunas², N. B. Suntzeff², M. Roth¹, L. Germany³,
P. Candia², S. Gonzalez¹, M. Hamuy⁴, W. L. Freedman⁴, S. E. Persson⁴, P. E.
Nugent⁵, G. Aldering⁵, and A. Conley⁵

¹ Las Campanas Observatory, Carnegie Observatories, Casilla 601, La Serena, Chile

² Cerro Tololo Inter-American Observatory, Casilla 603, La Serena, Chile

³ European Southern Observatory, Casilla 19001, Santiago 19, Chile

⁴ Observatories of the Carnegie Institution of Washington, 813 Santa Barbara Street,
Pasadena, CA 91101

⁵ Lawrence Berkeley National Laboratory, Mail Stop 50-232, 1 Cyclotron Road,
Berkeley, CA 94720

1 Introduction

Beginning in March 1999, we have carried out four major observing campaigns with the Swope 1.0 m and du Pont 2.5 m telescopes at the Las Campanas Observatory (LCO) to obtain near-IR light curves of supernovae (SNe) of all types. Data have been obtained for a total of 25 events, with approximately half of these corresponding to Type Ia supernovae (SNe Ia). These observations are part of a long-term collaborative program at LCO and Cerro Tololo Inter-American Observatory to investigate in detail the photometric properties of SNe Ia in the near-IR. These data will be used to study the physics of the explosions and to refine the usage of these objects as cosmological standard candles.

2 *JHK* Light Curve Morphology

Since the pioneering work of Elias and collaborators[1,2], the *JHK* light curves of SNe Ia have been known to be double-peaked. The secondary maximum occurs ~ 30 days after the first maximum, and is most prominent in the *J* band. This double-peaked morphology is also observed in the *I* band[3], and is a function of the decline rate parameter $\Delta m_{15}(B)$ [15] in the sense that the secondary maximum occurs later and also is generally stronger in the slowest-declining SNe Ia[6,18,10]. Except for the very fastest-declining events, the primary maximum in *I* occurs a few days *before* *B* maximum[6].

Fig. 1 shows plots of the *JHK* light curves of six SNe Ia covering a range of decline rates. Data for three of these SNe (1999aw, 2000bk, and 2001ba) were obtained as part of our observing program; photometry for the other three (1981B, 1986G, and 1998bu) are taken from the literature[1,5,12,7,9]. As in the *I* band, we see that 1) the secondary maximum occurs later for the slower-declining events, and 2) the primary maximum occurs a few days before *B* maximum. The dip between the primary and secondary maxima is much less pronounced in the *H* and *K* bands than in *J*, and the secondary maxima reach nearly the same

magnitude as the primary maxima in these two bands. The net effect is that the H and K light curves are fairly flat from a few days before B maximum to 20-35 days after.

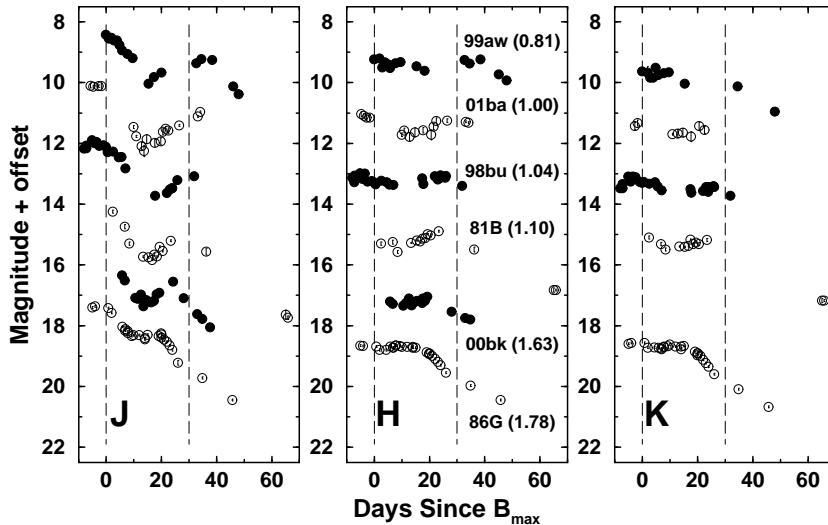


Fig. 1. JHK light curves of SNe Ia representing a range of decline rates. The curves have been arbitrarily shifted in magnitude with respect to each other for the purposes of comparison. The value of $\Delta m_{15}(B)$ is given in parentheses after the name of the SN. Dashed lines are drawn at 0 and 30 days past B maximum to serve as points of reference for the timing of the primary and secondary maxima.

We have also observed a few SNe Ia in the Y band at $1.035 \mu\text{m}$ [8]. At this wavelength – between the I and J bands – the secondary maximum is extremely prominent and, at least in some cases, brighter than the primary maximum. (The Z -band light curve of SN 1999ee shows a similar behavior[19].) We intend to continue collecting data in the Y band for future SNe Ia.

3 Absolute Magnitudes

In the top three panels of Fig. 2 we plot the absolute magnitudes in BVI versus the decline rate parameter $\Delta m_{15}(B)$ for two samples of SNe Ia. The first consists of 16 well-observed nearby SNe Ia which have occurred in host galaxies for which distances have been derived via Cepheids or the surface brightness fluctuations, planetary nebula luminosity function, or “tip of the red giant branch” methods. The calibration for all four methods is based on final results of the HST Key Project to measure the Hubble constant[4]. The second sample consists of 50 SNe Ia in the Hubble flow (i.e. with redshifts greater than 3000 km s^{-1}). Distances for these objects were derived from the host galaxy recession velocity

assuming $H_0 = 74 \text{ km s}^{-1} \text{ Mpc}^{-1}$ which gives the best agreement between the two samples. The bottom panel shows the absolute H magnitudes at 10 days after B maximum for the few SNe in the two samples with H -band light curves. This epoch was selected rather than maximum light which occurs several days before B maximum and therefore has been observed for very few SNe Ia. Note that all of the data plotted in Fig. 2 have been corrected for both Galactic and host galaxy reddening[17].

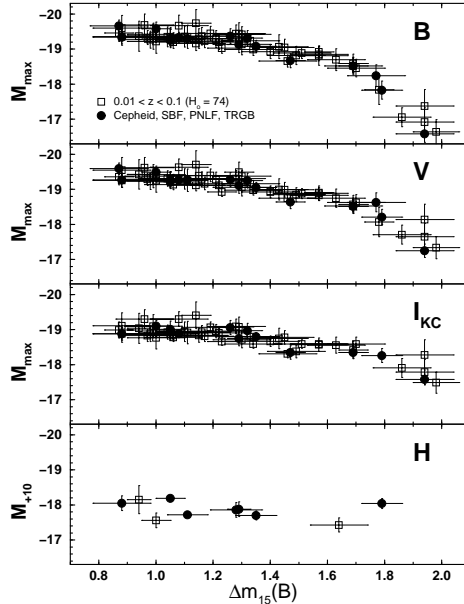


Fig. 2. Absolute magnitudes in $BVIH$ versus $\Delta m_{15}(B)$ for 66 well-observed SNe Ia.

In H , the slope of the luminosity versus decline rate relation appears to be essentially flat for $0.8 < \Delta m_{15}(B) < 1.4$. For the six nearby SNe with independent distance determinations in this range, we find a weighted mean H -band absolute magnitude at $t = +10$ days of $M(H_{+10}) = -17.91 \pm 0.05$. Interestingly, the absolute magnitudes of the two SNe Ia with $\Delta m_{15}(B) > 1.4$ are consistent with this value suggesting that the near-IR luminosities of SNe Ia may have little or no dependence on the decline rate (see also [13]). Further observations are obviously required to confirm this result.

4 Hubble Diagram

One of the great advantages of working in the near-IR is the minimal effect of dust reddening ($A_H \sim 0.1 A_B$). If the absolute magnitudes of SNe Ia in the near-IR are essentially independent of the decline rate, these objects would then

be nearly perfect standard candles at these wavelengths. Hubble diagrams in V and H for seven SNe Ia in the Hubble flow ($z > 0.01$) are shown in Fig. 3. For the V band we have corrected for Galactic and host galaxy extinction, and also for the absolute magnitude versus decline rate relation[17]. The HST Key Project Cepheid distances[4] are assumed for the calibration of the SNe Ia absolute magnitudes. A Hubble constant of 73 ± 4 km s $^{-1}$ Mpc $^{-1}$ is obtained with a small dispersion (0.08 mag), consistent with previous results[17].

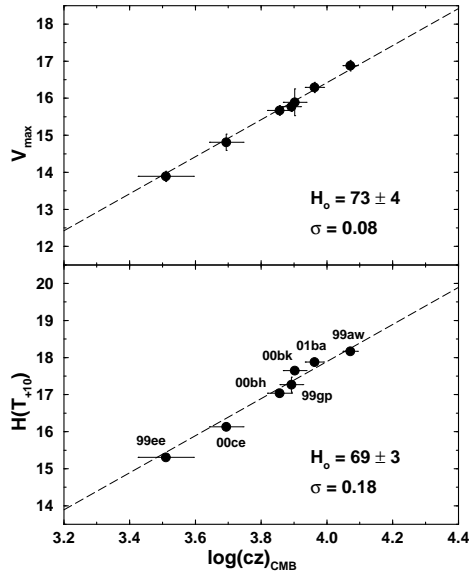


Fig. 3. V and H band Hubble diagrams for seven SNe Ia with $z > 0.01$.

For the H -band points in Fig. 3 we again use the magnitudes at 10 days after B maximum. These have been corrected for dust extinction using the same reddenings assumed for the V data, but no correction has been made for any possible dependence of absolute magnitude on decline rate. A Hubble constant of 69 ± 3 km s $^{-1}$ Mpc $^{-1}$ is implied assuming the value of $M(H_{+10})$ derived in Sect. 3. This agrees to within the errors with the value obtained from the V diagram, although the dispersion of 0.18 mag is a factor of two greater. There are at least two (possibly related) reasons why this might be the case: 1) The H band measurements were made at 10 days after B maximum and the scatter at this epoch may be greater due to the dependence of the light curve shape on the decline rate, and 2) the assumption of a constant absolute magnitude as a function of the decline rate may be incorrect. These hypotheses can only be tested by obtaining more near-IR light curves of SNe Ia which include the maximum-light epoch. Nevertheless, the consistency between the Hubble constants derived independently from the optical and IR data in Fig. 3 already suggests that the

methods developed for correcting the optical data for host galaxy reddening and decline rate effects are basically sound.

5 Interesting Objects

5.1 SN 1999ac

SN 1999ac was one of the first SN Ia observed in our program. As shown in Fig. 4, our optical and near-IR light curves begin ~ 2 weeks before B maximum, making them among the most detailed ever obtained of a SN Ia. Spectra taken before maximum indicated that this SN was a “peculiar” event similar to SNe 1991T and 1999aa[16]. The optical light curves of SN 1999ac were also peculiar – in particular, the B light curve displayed a slow rise to maximum similar to the light curve of SN 1991T, but then declined much more rapidly than 1991T. These photometric peculiarities make it difficult to estimate the host galaxy reddening via standard techniques.

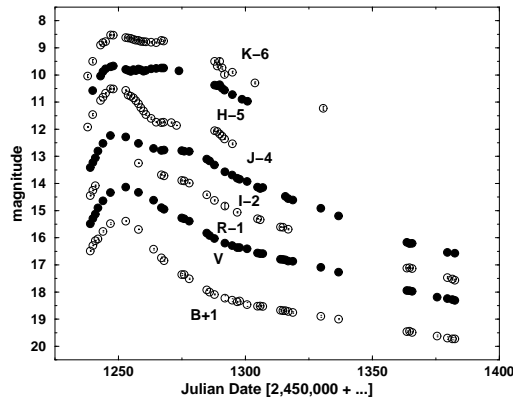


Fig. 4. $BVRIJK$ light curves of SN 1999ac.

5.2 SN 2001ay

SN 2001ay appeared in the early-type spiral galaxy IC 4423. A spectrum obtained near maximum indicated that the ejecta had unusually high expansion velocities[11]. Fig. 5 shows our $UBVRIJK$ light photometry compared with template curves for a “typical” SN Ia. The decline rate of 2001ay ($\Delta m_{15}(B) \sim 0.6-0.7$) is the slowest that we have ever observed. Note the plateau character of the I and J light curves with no strong dip between the two maxima. It is not clear if this photometric peculiarity is related to the high ejecta velocities, or is simply a characteristic of all SNe Ia with such slow decline rates. As in the case of

SN 1999ac, we cannot use standard methods to derive the host galaxy extinction of SN 2001ay, but this is likely to have been fairly small ($E(B - V) \leq 0.1$) since an echelle spectrum[14] showed Na I D lines at the redshift of IC 4423 which are no stronger than those due to the Milky Way. This implies $M(V_{max}) \sim -19.2$, which is surprisingly low for such a slow-declining SN Ia. On the other hand, in the near-IR this object was significantly more luminous ($M(H_{+10}) \sim -18.6$) than the other SNe Ia we have observed to date (see Sect. 3).

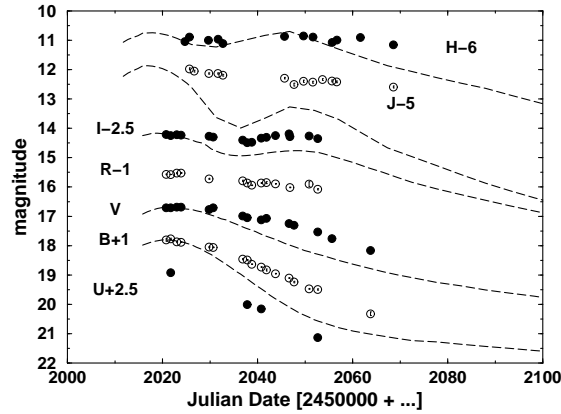


Fig. 5. *UBVRIJH* light curves of SN 2001ay. Dashed lines show template light curves of a “typical” SN Ia.

References

1. J.H. Elias, et al.: ApJ **251**, L13 (1981)
2. J.H. Elias, et al.: ApJ **296**, 379 (1985)
3. C.H. Ford, et al.: AJ **106**, 1101 (1993)
4. W.L. Freedman, et al.: Astrophys. J. **553**, 47 (2001)
5. J.A. Frogel, et al.: ApJ **315**, L129 (1987)
6. M. Hamuy, et al.: AJ **112**, 2438 (1996)
7. M. Hernandez, et al.: MNRAS **319**, 223 (2000)
8. L.A. Hillenbrand, et al.: PASP **114**, 708 (2002)
9. S. Jha, et al.: ApJS **125**, 73 (1999)
10. K. Krisciunas et al.: AJ **122**, 1616 (2001)
11. T. Matheson, et al.: IAU Circ. 7612 (2001)
12. Y.D. Mayya, I. Puerari, O. Kuhn: IAU Circ. 6905 (1998)
13. W.P.S. Meikle: MNRAS **314**, 782 (2000)
14. P. Nugent, et al.: IAU Circ. 7612 (2001)
15. M.M. Phillips: Astrophys. J. **413**, L105 (1993)
16. M.M. Phillips, A.V. Filippenko: IAU Circ. 7122 (1999)
17. M.M. Phillips, et al.: AJ **118**, 1766 (1999)
18. A.G. Riess, W.H. Press, R.P. Kirshner: ApJ **473**, 88 (1996)
19. M. Stritzinger, et al.: AJ **124**, 2100 (2002)